Article

Molecular Cell

Delayed Accumulation of H3K27me3 on Nascent DNA Is Essential for Recruitment of Transcription Factors at Early Stages of Stem Cell Differentiation

Graphical Abstract

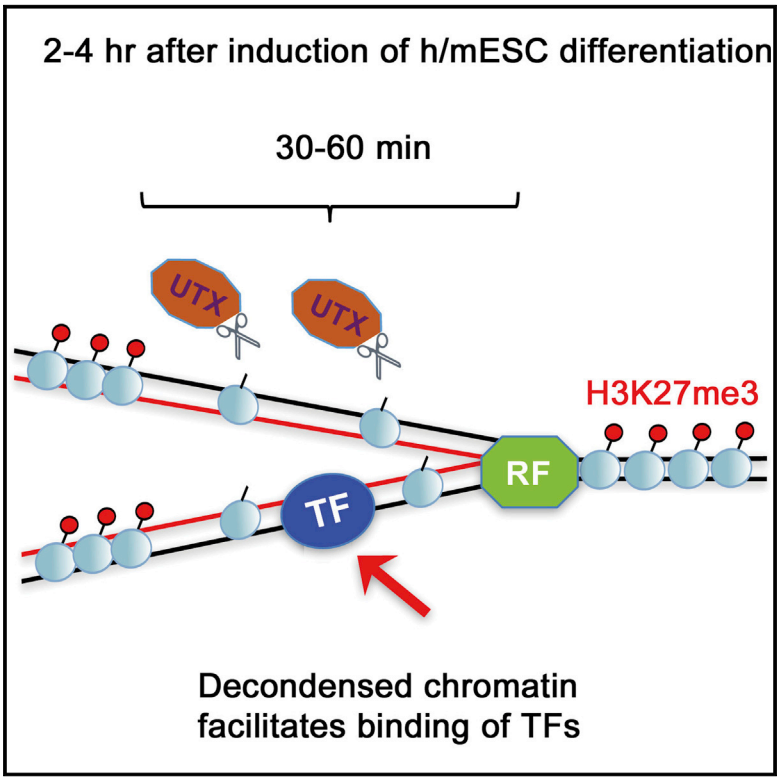

Highlights

- Induction of h/mESCs leads to increased association of UTX with nascent DNA
- UTX prevents methylation of H3K27me3, creating a temporal window of "open" chromatin
- "Open" nascent chromatin allows recruitment of lineage-specifying TFs to DNA
- Blocking DNA replication or inhibiting UTX prevents association of TFs with DNA

Authors

Svetlana Petruk, Jingli Cai, Robyn Sussman, ..., Hugh W. Brock, Lorraine Iacovitti, Alexander Mazo

Correspondence

lorraine.iacovitti@jefferson.edu (L.I.), alexander.mazo@jefferson.edu (A.M.)

In Brief

Recruitment of TFs, including pioneer factors, is impeded by condensed H3K27me3-containing chromatin. Petruk et al. find that, following induction of ESC differentiation, accumulation of the repressive histone mark H3K27me3 is delayed after DNA replication, thus providing a "window of opportunity" for recruitment of lineage-specific TFs to nascent DNA.

Petruk et al., 2017, Molecular Cell 66, 247–257
April 20, 2017
http://dx.doi.org/10.1016/j.molcel.2017.03.006

CellPress

Molecular Cell
Article

Delayed Accumulation of H3K27me3 on Nascent DNA Is Essential for Recruitment of Transcription Factors at Early Stages of Stem Cell Differentiation

Svetlana Petruk,[1,5] Jingli Cai,[2,5] Robyn Sussman,[3,6] Guizhi Sun,[1] Sina K. Kovermann,[4] Samanta A. Mariani,[3,7] Bruno Calabretta,[3] Steven B. McMahon,[3] Hugh W. Brock,[4] Lorraine Iacovitti,[2,*] and Alexander Mazo[1,8,*]
[1]Department of Biochemistry and Molecular Biology
[2]Department of Neuroscience
[3]Department of Cancer Biology
Sidney Kimmel Medical College, Sidney Kimmel Cancer Center, Thomas Jefferson University, Philadelphia, PA 19107, USA
[4]Department of Zoology, University of British Columbia, 6270 University Boulevard, Vancouver, BC V6T 1Z4, Canada
[5]Co-first author
[6]Present address: Division of Oncology and Center for Childhood Cancer Research, Children's Hospital of Philadelphia, Philadelphia, PA 19104, USA
[7]Present address: Center for Inflammation Research, Queen's Medical Research Institute, University of Edinburgh, Edinburgh EH16 4TJ, Scotland
[8]Lead Contact
*Correspondence: lorraine.iacovitti@jefferson.edu (L.I.), alexander.mazo@jefferson.edu (A.M.)
http://dx.doi.org/10.1016/j.molcel.2017.03.006

SUMMARY

Recruitment of transcription factors (TFs) to repressed genes in euchromatin is essential to activate new transcriptional programs during cell differentiation. However, recruitment of all TFs, including pioneer factors, is impeded by condensed H3K27me3-containing chromatin. Single-cell and gene-specific analyses revealed that, during the first hours of induction of differentiation of mammalian embryonic stem cells (ESCs), accumulation of the repressive histone mark H3K27me3 is delayed after DNA replication, indicative of a decondensed chromatin structure in all regions of the replicating genome. This delay provides a critical "window of opportunity" for recruitment of lineage-specific TFs to DNA. Increasing the levels of post-replicative H3K27me3 or preventing S phase entry inhibited recruitment of new TFs to DNA and significantly blocked cell differentiation. These findings suggest that recruitment of lineage-specifying TFs occurs soon after replication and is facilitated by a decondensed chromatin structure. This insight may explain the developmental plasticity of stem cells and facilitate their exploitation for therapeutic purposes.

INTRODUCTION

Differentiation of embryonic stem cells (ESCs) into differentiated cell types is both a fundamental biological process and central for developing new therapeutic tools for many diseases. Stem cell differentiation is triggered by lineage-specific inducers whose binding brings about well characterized massive changes in the transcriptome and epigenome (Sha and Boyer, 2008). Many key genes that are induced during cell differentiation are either repressed or poised for future activation by possessing bivalent chromatin domains in uninduced pluripotent cells.

The structure of chromatin creates a barrier for the association of newly induced transcription factors (TFs) with their sites on DNA. Many TFs cannot bind the L-type chromatin (Iwafuchi-Doi and Zaret, 2016), which contains nucleosomes without many activating or repressive marks (Kharchenko et al., 2011; Kundaje et al., 2015). However, a group of TFs called pioneer factors are able to bind to DNA in the L regions of chromatin and to facilitate binding of other essential TFs (Gualdi et al., 1996; Iwafuchi-Doi and Zaret, 2014; Zaret, 1999; Zaret and Carroll, 2011). In contrast, actively repressed chromatin (R-type) is not accessible to any TFs, including pioneer factors (Iwafuchi-Doi and Zaret, 2016). This chromatin includes essential repressed and poised/bivalent genes in the euchromatin that are marked by H3K27me3 and that have to be activated during induction of undifferentiated ESCs. Although the "pioneer factor" mechanism provides an attractive explanation of how some TFs may overcome chromatin barriers in particular regions of the genome, it does not provide a universal explanation for all essential TFs in all regulatory regions during differentiation of stem cells. Thus, the mechanism of gene activation during differentiation of stem cells remains enigmatic.

The key assumption in this field is that the chromatin structure is always condensed/tight at the time of recruitment of TFs. However, because most studies of TF binding use bulk chromatin before and after induction of cell differentiation that consists largely of transcriptional interphase chromatin, to our knowledge, no one has determined the chromatin status during TF binding. There is no a priori reason to believe that the structure of the interphase chromatin is more amenable to recruitment of newly induced TFs. On the other hand, the structure of chromatin is thought to be completely re-established during DNA replication

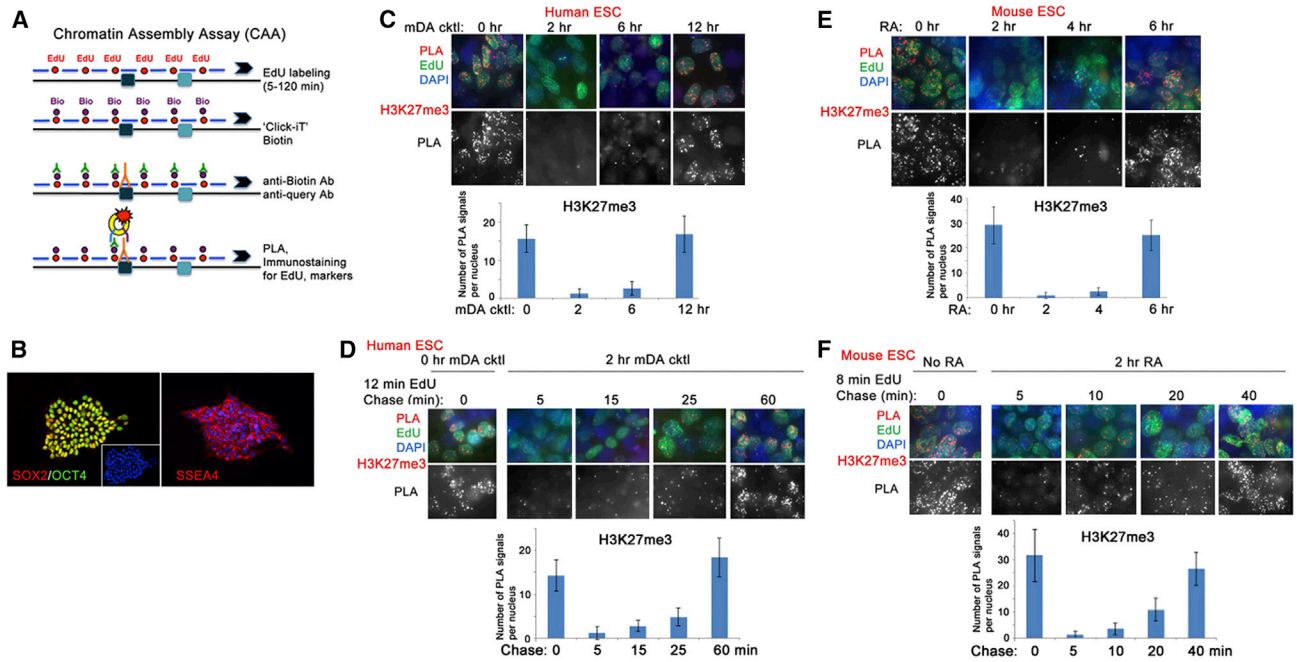

Figure 1. Accumulation of H3K27me3 in Single Cells following DNA Replication during Induction of Differentiation of hESCs and mESCs

(A) A scheme of the CAA (Petruk et al., 2012). Bio, biotin.

(B) Immunostaining of uninduced hESC colonies in stage 1 medium with antibodies to SOX2 (red), OCT4 (green), and DAPI (blue in the inset) on the left and SSEA4 (red) and DAPI on the right.

(C) hESCs were grown for 4 days in stage 1 medium and then induced with the mDA cocktail to the mDA lineage for the indicated times. Cells were labeled with EdU for 15 min.

(D) hESCs were grown for 4 days in stage 1 medium and then induced for 2 hr with the mDA cocktail. Cells were labeled with EdU for 12 min and chased for the indicated times.

(E) mESCs were induced with RA for the indicated times. Cells were labeled with EdU for 12 min.

(F) mESCs were induced with RA for 2 hr. Cells were labeled with EdU for 8 min and chased for the indicated times.

In (C)–(F), CAA was performed for H3K27me3, followed by immunostaining for biotin (EdU). PLA, red; biotin, green; DAPI, blue. PLA only is shown in black and white. Quantification of the results of three independent CAA experiments is shown below.

and, therefore, may present an opportunity for easy association of new protein molecules. Thus, the molecular events following DNA replication may be essential for understanding changes in transcriptional programs during differentiation.

Current techniques that allow analysis of the structure of nascent chromatin are limited. Recent mass spectrometry-based approaches, isolate proteins on nascent DNA (iPOND) (Sirbu et al., 2012) and nascent chromatin capture (NCC) (Alabert et al., 2014), are based on identification of proteins that are associated with newly replicated DNA. However, these techniques require large amounts of homogeneous synchronized cells. We developed the chromatin assembly assay (CAA), the only method currently available that allows examination of proteins associated with nascent DNA following replication in single cells (Petruk et al., 2012; scheme in Figure 1A). This method is based on the proximity ligation assay (PLA) and, therefore, provides a unimolecular sensitivity in the examination of the association of proteins with nascent DNA after replication in vivo. The kinetics of the accumulation of proteins on nascent DNA can also be examined at a gene-specific level by a complementary method, sequential chromatin immunoprecipitation (re-ChIP) with bromodeoxyuridine (BrdU)-labeled DNA (Francis et al., 2009; Petruk et al., 2012).

We used the CAA and re-ChIP with BrdU-labeled DNA methodologies to gain an understanding of how new transcriptional programs are established at a single-cell level and at a gene-specific level, respectively, during early stages of differentiation of human (hESCs) and mouse ESCs (mESCs). We found a new chromatin-based feature of ESCs that is essential for the early stages of differentiation of these cells. The structure of post-replicative chromatin undergoes significant changes during the first several hours following induction of differentiation of mESCs and hESCs. Accumulation of the histone H3K27me3, which marks both repressed and bivalent euchromatic genes in undifferentiated ESCs, on nascent DNA is delayed during the very early stages of ESC differentiation. Because the absence of H3K27me3 is known to coincide with a less condensed structure of nucleosomes (Bell et al., 2010; Shlyueva et al., 2014; Yuan et al., 2012), this may create a critical opportunity for the recruitment of newly induced TFs, including pioneer TFs, to DNA. We propose that the new chromatin-based feature of ESCs is essential for the early stages of differentiation of these cells. Our findings may provide a molecular explanation for the developmental plasticity of ESCs and lead to the development of more efficient ways to differentiate stem cells into desired lineages for potential therapeutic use.

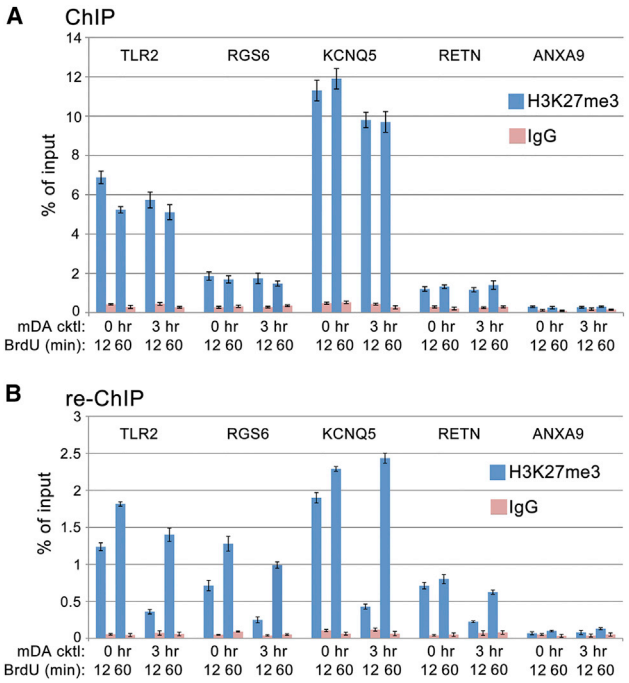

Figure 2. Accumulation of H3K27me3 on Nascent DNA of Specific Genes during Neuronal Differentiation of hESCs

(A) Uninduced hESCs and hESCs induced for 3 hr with the mDA cocktail were labeled with BrdU for 12 min or for 12 min followed by a chase to 60 min. Chromatin was first immunoprecipitated with H3K27me3 and immunoglobulin G (IgG) antibodies. qPCR was performed at the H3K27me3-containing genes TLR2, RGS6, KCNQ5, and RETN and at one control gene, ANXA9, which does not contain H3K27me3 according to Pan et al. (2007).

(B) In the second step, DNA purified from the resulting material of the first immunoprecipitation step with H3K27me3 antibody was immunoprecipitated with the BrdU antibody and PCR-amplified at the same regions as in (A). The percent of input for re-ChIP experiments was calculated using the amount of material eluted from the beads following immunoprecipitation with H3K27me3 as 100% input.

Data are represented as mean ± SEM.

RESULTS

A Time Window of Delayed Accumulation of Post-replicative H3K27me3 during the Early Stages of ESC Differentiation

How any transcription factor overcomes the barrier of the most condensed chromatin to bind to DNA and to change transcriptional programs during cell differentiation is not well established. However, it is thought that the chromatin structure is disrupted and then re-assembled following DNA replication (Bonasio et al., 2010; Corpet and Almouzni, 2009). Therefore, we examined whether, during the early periods after DNA replication, the structure of chromatin that is formed on nascent DNA may provide an opportunity for newly induced transcription factors to overcome the barrier of condensed chromatin and associate with their target sites on DNA. In this study, we focused on the events that occur during the first several hours following induction of differentiation in mammalian ESCs using two well established differentiation protocols (Chung et al., 2009; Prakash and Wurst, 2007).

Using our previously developed CAA approach (Petruk et al., 2012; scheme in Figure 1A), we found that the rate of accumulation of the repressive histone mark H3K27me3 on nascent DNA just after replication drastically changes during the earliest stages of differentiation of hESCs and mESCs. The undifferentiated hESCs that express the pluripotency markers SOX2, OCT4, and SSEA4 (Figure 1B) exhibit rapid (10–15 min) and robust accumulation of H3K27me3 on newly replicated DNA (Figure 1C). Surprisingly, treatment with a cocktail of factors that promotes midbrain dopamine neuronal (mDA) differentiation in human stem cells (Cai et al., 2013; Kriks et al., 2011) led to a very significant decrease in the accumulation of H3K27me3 after DNA replication. Compared with 12 PLA signals for H3K27me3 per EdU-labeled nucleus detected in uninduced cells, we detected either no or occasional signals in hESCs induced with the mDA cocktail for 2 and 6 hr (Figure 1C). This robust, quantitative distinction was consistently observed over the course of numerous experiments, as presented below. During the period of delay in the accumulation of post-replicative H3K27me3, there was an insignificant amount of H3K27me3 on nascent DNA for at least 30–40 min after DNA replication in hESCs (Figure 1D). This result is consistent with our previous finding that accumulation of H3K27me3 is delayed by at least 1 hr following DNA replication in rapidly differentiating cells of early *Drosophila* embryos (Petruk et al., 2012). Interestingly, the fast (10–15 min) and widespread mode of accumulation of H3K27me3 returns following 12 hr of induction of hESC differentiation (Figure 1C).

The results with undifferentiated mESCs that were induced with retinoic acid (RA) were in general very similar to the results in hESCs. From 2–4 hr after induction with RA, accumulation of H3K27me3 after DNA replication is delayed by 30 min (Figures 1E and 1F). We conclude that, during the early stages of ESC differentiation, the mode of accumulation of H3K27me3 after DNA replication undergoes significant changes. Prior to induction of differentiation, undifferentiated hESCs and mESCs possess a very rapid mode of H3K27me3 accumulation. During several hours following induction of differentiation to a specific lineage, accumulation of H3K27me3 significantly slows down and then returns to the fast mode about 6–12 hr after induction. A shorter cell cycle of mESCs (12 hr in mESCs versus 16 hr in hESCs) (Barta et al., 2013; Li et al., 2012) may explain why we observed a return of rapid accumulation of H3K27me3 in mESCs compared with hESCs (Figures 1C and 1E).

To confirm these findings for specific genes, we analyzed the kinetics of accumulation of H3K27me3 on nascent DNA before and 3 hr after induction of mDA differentiation in hESCs by re-ChIP assays with BrdU-labeled DNA (Francis et al., 2009; Petruk et al., 2012). These assays were performed following labeling of DNA with BrdU for 12 min, followed by no chase or a chase to 1 hr. Chromatin was cross-linked, sonicated, and immunoprecipitated with antibody to H3K27me3 (ChIP in Figure 2A). DNA was then purified and immunoprecipitated with antibody to BrdU (re-ChIP in Figure 2B). Given our goal of investigating changes in the kinetics of accumulation of H3K27me3 on nascent DNA before and after induction of hESC differentiation, for this analysis, we were obliged to analyze genes that are repressed in pluripotent cells and that remain repressed following induction of hESCs because active genes would be

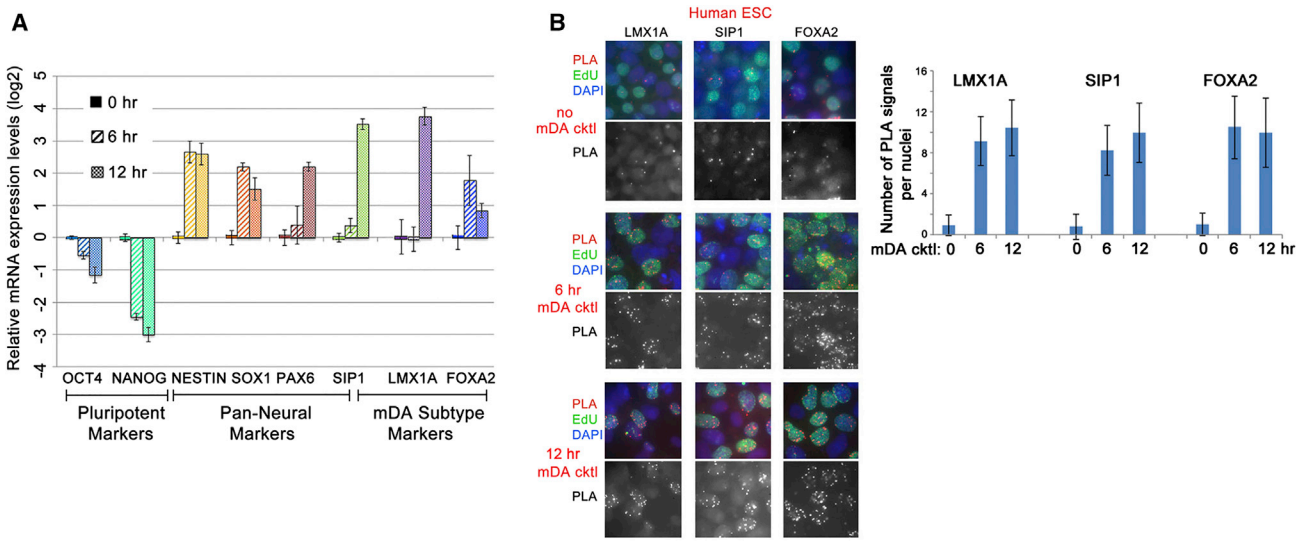

Figure 3. Induction of Expression and Association with DNA of Lineage-Specific TFs during mDA Differentiation of hESCs

(A) qRT-PCR gene expression analysis of undifferentiated (0 hr, control) hESCs and hESCs induced to the mDA lineage for 6 and 12 hr.

(B) Undifferentiated hESCs (top) and hESCs induced to the mDA lineage for 6 hr (bottom) were labeled with EdU for 15 min and then chased for 15 min. CAA was performed for LMX1A, FOXA2, and SIP1, followed by immunostaining for biotin (green). PLA only is shown in black and white. Quantification of the results of three independent CAA experiments is also shown (right).

expected to lose H3K27me3. These genes are either repressed and contain only H3K27me3 (TLR2) or are bivalent and contain both H3K27me3 and H3K4me3 in their regulatory regions (RGS6, KCNQ5, and RETN) (Pan et al., 2007). The results of conventional ChIP assays (Figure 2A) confirm the association of H3K27me3 with the regulatory regions of all tested genes compared with the control ANXA9 gene that is activated and does not contain H3K27me3 (Pan et al., 2007). Prior to induction of differentiation, significant levels of H3K27me3 were detected by the re-ChIP assays on nascent DNA labeled for 12 min with a slight increase following the chase to 60 min (Figure 2B). However, 3 hr following induction of hESC differentiation with the mDA cocktail, the amounts of H3K27me3 on 12-min-labeled nascent DNA were very low, and they significantly increased following chase to 60 min (Figure 2B). This demonstrates that, compared with uninduced cells, the accumulation of H3K27me3 on nascent DNA of specific genes is temporarily delayed following induction of hESC differentiation. Thus, the results of the gene-specific re-ChIP assays provide an independent confirmation of the results of the single-cell CAAs and demonstrate the same mode of delayed accumulation of H3K27me3 on nascent DNA at both repressed and bivalent genes following induction of hESC differentiation.

Key Fate-Specifying TFs Are Associated with Nascent DNA within Hours after Induction of ESC Differentiation

The above results suggest that, following induction of differentiation, the genomes of stem cells switch from rapid to slow accumulation of H3K27me3 on nascent DNA so that, just after replication, the newly deposited nucleosomes at any gene are devoid of the repressive H3K27me3 histone mark. Importantly, a high content of nucleosomes with H3K27me3 correlates with a high density of nucleosomes and low accessibility of DNA (Bell et al., 2010; Yuan et al., 2012). The absence of H3K27me3 during the early stages of replication of induced stem cells may lead to a lower density of nucleosomes and higher accessibility of DNA on the newly synthesized DNA.

We hypothesized that this chromatin structure could facilitate recruitment to DNA of TFs that are induced in response to differentiation stimuli. However, induction of differentiation-specific TFs within a few hours of ESC differentiation has not been demonstrated previously. We used qRT-PCR analysis to show that mRNA levels of the pluripotency markers OCT4 and NANOG decrease and the mRNA levels of the pan-neural markers NESTIN, SOX1, and PAX6 and the pan-neural and mDA subtype marker SIP1 (Cai et al., 2013) increase as early as 6–12 hr after induction of hESCs to the mDA lineage (Figure 3A). Using CAA, we found that the SIP1 transcription factor is not associated with DNA within 30 min after replication in uninduced hESCs and is first detected on nascent DNA after 6 hr of stem cell differentiation (Figure 3B). Surprisingly, even LMX1A and FOXA2, TFs associated specifically with the mDA neuronal subtype (Cai et al., 2009; Chung et al., 2009; Prakash and Wurst, 2007), are detected in hESCs by CAA 6 hr after induction of hESC differentiation (Figure 3B). Induction of expression of SIP1 and FOXA2 at 6 hr was confirmed by qRT-PCR (Figure 3A); the low level of LMX1 RNA at 6 hr by qRT-PCR may be caused by the lower sensitivity of this assay compared with the PLA or by a relatively lower level of expression of this gene at this time point. These results indicate that the neuronal subtype may be determined far earlier than previously thought and suggest that both primary (i.e., neural) and secondary (neuronal subtypes) fate choices are made within hours of the initiation of the differentiation process of hESCs in culture.

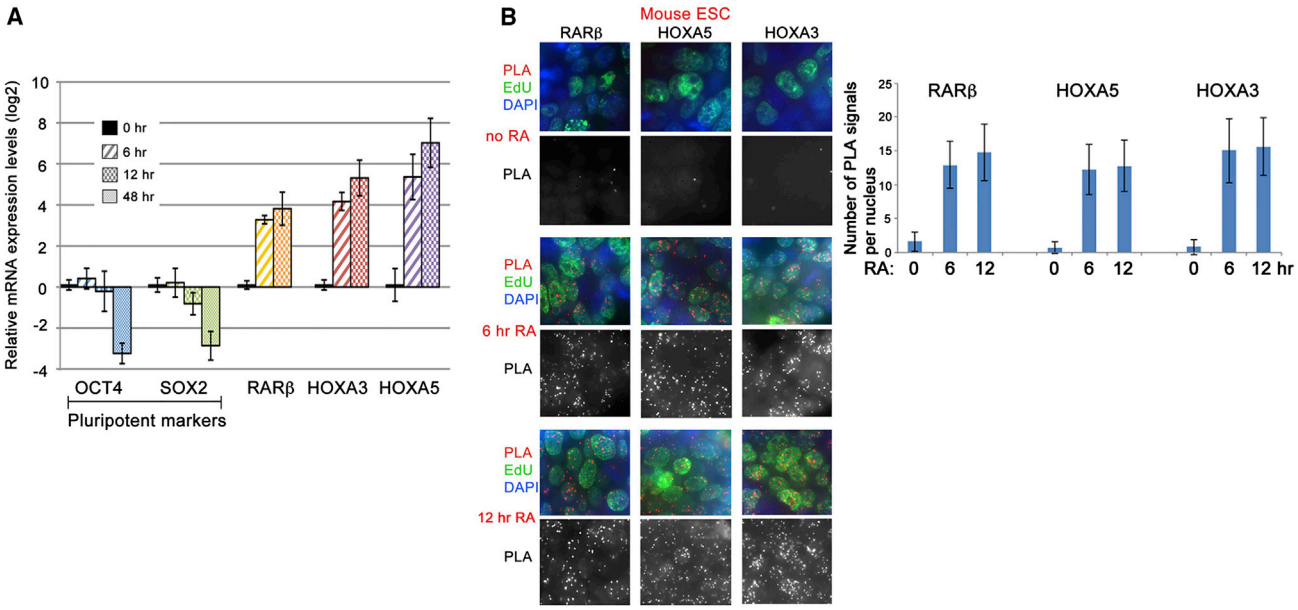

Figure 4. Association with DNA of Newly Induced TFs during Induction of Differentiation of mESCs

(A) qRT-RCR gene expression analysis of undifferentiated (0 hr, control) mESCs and mESCs induced with RA for the indicated times.

(B) mESCs were induced with RA for 6 hr. Cells were labeled with EdU for 15 min and then chased for 15 min. CAA was performed for RARβ, HOXA5, and HOXA3, followed by immunostaining for biotin (green). PLA only is shown in black and white. Quantification of the results of three independent CAA experiments is also shown (right).

We also induced differentiation of mESCs and tested the expression and association with DNA of the proteins that are expressed following induction with RA. qRT-PCR assays show that RARβ, HOXA5, and HOXA3 RNAs are induced 6 hr following treatment with RA (Figure 4A), as shown previously (Al Tanoury et al., 2014; Rochette-Egly, 2015; Simandi et al., 2010). CAA demonstrates that the corresponding proteins are not associated with DNA prior to induction of differentiation (Figure 4B). After 6 hr of induction with RA, we detected significant amounts of RARβ, HOXA5, and HOXA3 on nascent DNA 30 min after replication (Figure 4B). The amount of RNA or PLA signals for the TFs examined in hESCs and mESCs is not increased from 6–12 hr after induction of differentiation of both hESCs and mESCs (Figures 3B and 4B), suggesting that accumulation of early induced proteins on nascent DNA occurs mostly during the time period when post-replicative DNA contains very low numbers of nucleosomes with H3K27me3.

DNA Replication Is Essential for Recruitment of TFs to DNA

Knowledge of the cell-cycle stage at which TFs are recruited to DNA is generally important because the mechanisms and the cell-cycle stage of the initial recruitment of newly induced TFs, and thus the acquisition of differentiation signals, are poorly understood. Although it was proposed that recruitment of TFs occurs in the G1 phase (Kapinas et al., 2013; Murray and Kirschner, 1989; Singh and Dalton, 2009), this model is not fully supported by experimental data (Filipczyk et al., 2007; Jonk et al., 1992; Li et al., 2012; Mummery et al., 1987). The results above led us to examine whether TF recruitment to DNA occurs exclusively during the early post-replication stages.

To test our hypothesis, hESCs and mESCs were labeled with EdU for 30 min to allow further analysis by CAA. Then EdU-labeled cells were induced with the mDA cocktail or RA in the presence of thymidine and grown for 24 hr to prevent S phase entry. Twenty-four hour treatment with thymidine efficiently blocked DNA replication, and removal of thymidine for 4 hr restored DNA replication (Figures 5A and 5B, right). Blocking DNA replication with thymidine completely prevented association of LMX1A, SIP1, and FOXA2 with DNA in hESCs and RARβ, HOXA5, and HOXA3 in mESCs 24 hr following induction of differentiation (Figures 5A and 5B). Re-initiation of DNA synthesis 4 hr after release of the thymidine block leads to efficient recruitment of these TFs to DNA (Figures 5A and 5B). These results suggest that recruitment of TFs following induction of differentiation of hESCs and mESCs occurs exclusively during the early periods after DNA replication. The amounts of TFs associated with nascent DNA do not increase from 6–12 hr after induction of differentiation (Figures 3B and 4B), suggesting that these proteins are not significantly recruited to DNA during the remainder of the cell cycle.

Accumulation of H3K27me3 on Nascent DNA Blocks Recruitment of Key TFs to DNA

To test our hypothesis that low global levels of H3K27me3 in post-replicative chromatin are essential for recruitment of TFs to DNA, we examined whether raising the levels of H3K27me3 on nascent DNA reduced the recruitment of lineage-specifying TFs. We found previously that inhibiting the H3K27me3 lysine

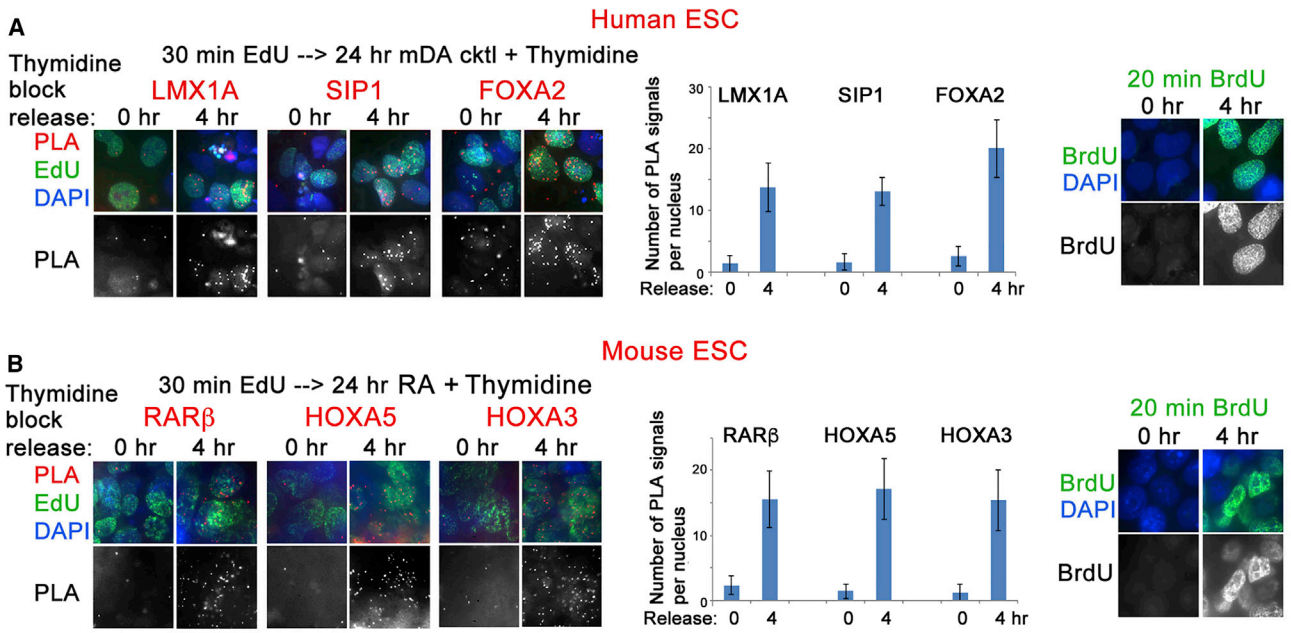

Figure 5. Lineage-Specific TFs Associate with DNA Shortly after DNA Replication

(A) hESCs were grown for 4 days in stage 1 medium and labeled with EdU for 30 min. Cells were induced to the mDA lineage and grown for 24 hr in the presence of thymidine. The thymidine block was removed for 0 hr (left) and 4 hr (right). CAA was performed for LMX1A, FOXA2, and SIP1, followed by immunostaining for biotin (green). PLA only is shown in black and white. Thymidine block release was monitored by 20-min incorporation of BrdU (green, right). Quantification of the results of three independent CAA experiments is shown in the center.

(B) mESCs were grown for 2 days with leukemia inhibitory factor (LIF)/2i and labeled with EdU for 30 min. Cells were induced with RA and grown for 24 hr in the presence of thymidine. The thymidine block was removed for 0 hr (left) and 4 hr (right). CAA was performed for RARβ, HOXA5, and HOXA3, followed by immunostaining for biotin (green). PLA only is shown in black and white. Thymidine block release was monitored by 20-min incorporation of BrdU (green, right). Quantification of the results of three independent CAA experiments is shown in the center.

demethylases (KDMs) UTX and JMJD3 using GSKJ4 (Kruidenier et al., 2012) significantly accelerates the accumulation of H3K27me3 on nascent DNA in *Drosophila* (Petruk et al., 2013). Therefore, undifferentiated hESCs and mESCs were grown in the presence of GSKJ4 for 4 hr and then induced with the mDA cocktail or with RA, respectively, for another 2 hr. We detected significant accumulation of H3K27me315 min after DNA replication when both types of cells were exposed to GSKJ4 (Figures 6A and 6C) compared with no accumulation of H3K27me3 in cells grown in the absence of GSKJ4.

Moreover, treatment with GSKJ4 strongly inhibited recruitment of LMX1A, SIP1, and FOXA2 to nascent DNA in hESCs induced for 6 hr with the mDA cocktail (Figure 6B) and recruitment of RARβ, HOXA5, and HOXA3 to nascent DNA 6 hr following induction of mESCs with RA (Figure 6D). Control experiments suggest that inhibition of the recruitment of these factors to nascent DNA in both hESCs and mESCs is not caused by inhibition of the transcription of the corresponding genes by treatment with GSKJ4 (Figure 6E). Taken together, these results suggest that recruitment of essential TFs to DNA in induced hESCs and mESCs occurs during the early period of DNA replication and depends on delayed accumulation of H3K27me3 on nascent chromatin. These insights may be critical for the development of therapeutic strategies that rely on the directed differentiation of stem cells into specific classes of cells.

Association and Activity of the KDM UTX with Nascent DNA Is Essential for ESC Differentiation

Changes in the rate of accumulation of H3K27me3 on nascent DNA during the initial stages of ESC differentiation may depend on the relative activities and/or amounts of antagonistic enzymes, H3K27 lysine methyltransferases (KMTs), and KDMs. The major H3K27me3 KMT EZH2 and one of the two enzymatically active H3K27me3 KDMs, JMJD3, are present on DNA in significant amounts before induction of hESC and mESC differentiation (Figures 7A and 7B). Because we detected high amounts of H3K27me3 in uninduced ESCs (Figures 1 and 2), it is likely that the KDM activity of JMJD3 is not sufficient to significantly counteract the histone methyltransferase (HMT) activity of EZH2 before induction of differentiation of stem cells. The relative amounts of JMJD3 and EZH2 on DNA remain at the same level 2 and 6 hr following induction of differentiation (Figures 1, 7A, and 7B), when we detect very low amounts of H3K27me3 on nascent DNA. Together, these results suggest that JMJD3 is unlikely to play a major role in de-methylation of H3K27me3 at this period of ESC differentiation.

In contrast, the amount of another H3K27me3 KDM associated with DNA, UTX, significantly fluctuates during ESC differentiation: the amount of UTX associated with DNA is very low in undifferentiated hESCs and mESCs, and it is significantly increased 2 hr following induction of differentiation of these cells (Figures

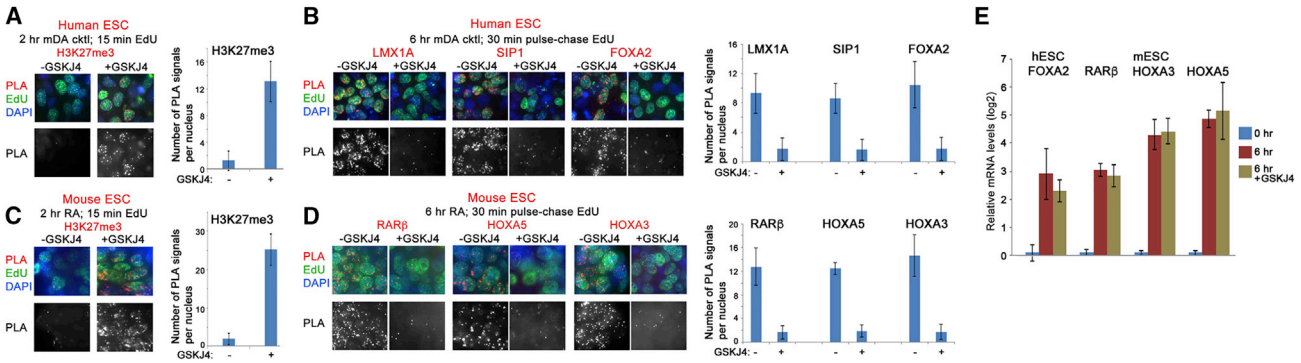

Figure 6. Lack of H3K27me3 in Post-replicative Chromatin Is Essential for the Association of Lineage-Specific TFs with DNA in mESCs and hESCs

(A) hESCs were grown in stage 1 medium for 4 days and then for 4 hr in the absence and presence of 10 μM GSKJ4 and induced to the mDA lineage for 2 hr. Cells were labeled with EdU for 15 min. CAA was performed for H3K27me3, followed by immunostaining for biotin (green). PLA only is shown in black and white.

(B) hESCs were grown and induced to the mDA lineage for 6 hr with and without GSKJ4. Cells were pulse-labeled with 5 μM EdU for 15 min and chased for 15 min. CAA was performed for LMX1A, SIP1, and FOXA2, followed by immunostaining for biotin (green). PLA only is shown in black and white.

(C) mESCs were grown for 2 days with LIF/2i and then for 4 hr in the absence and presence of 5 μM GSKJ4 and induced with RA for 2 hr. Cells were labeled with EdU for 15 min. CAA was performed for H3K27me3, followed by immunostaining for biotin (green). PLA only is shown in black and white.

(D) mESCs were grown for 2 days with LIF/2i and then induced with RA for 6 hr with and without GSKJ4. Cells were pulse-labeled with EdU for 15 min and chased for 15 min. CAA was performed for RARβ, HOXA5, and HOXA3, followed by immunostaining for biotin (green). PLA only is shown in black and white.

(E) qRT-PCR gene expression analysis of undifferentiated and induced hESCs and mESCs. hESCs were induced to the mDA lineage for 6 hr in the absence and presence of 10 μM GSKJ4. mESCs were induced with RA for 6 hr in the absence and presence of 5 μM GSKJ4.

In (A)–(D), quantification of the results of three independent CAA experiments is shown at the right.

7A and 7B). Because the amount of JMJD3 is not increased following induction of ESC differentiation, induced association of UTX 2 hr after induction of ESC differentiation may play a major role in the decreased amount of H3K27me3 on nascent DNA. These results are consistent with the possibility that a strong increase in the amount of chromatin-associated UTX masks the H3K27me3 activity of EZH2, leading to de-methylation of H3K27me3 on nascent DNA during the first several hours after induction of differentiation (Figures 1C, 1E, 7A, and 7B). This conclusion is supported by our previous finding that, despite the simultaneous presence of UTX and E(z) on DNA in undifferentiated cells of early *Drosophila* embryos, the activity of the HMT E(z) is masked by the activity of the KDM UTX (Petruk et al., 2013).

These conclusions are consistent with the fact that GSKJ4 inhibits enzymatic activities of both UTX and JMJD3. GSKJ4 does not affect the level of UTX in the nucleus (Figure 7D) or the association of UTX and EZH2 with DNA (Figure 7C), suggesting the absence of non-catalytic effects of UTX and indirect effects of this compound. Further, we investigated whether UTX is recruited to DNA following DNA replication, at the time of delayed accumulation of H3K27me3 and recruitment of TFs. Blocking DNA replication with thymidine did not affect the association of UTX with DNA, suggesting that this protein can be recruited before DNA replication (Figure 7E). The importance of UTX KDM activity at the early stages of differentiation is supported by the fact that inhibiting this enzyme with GSKJ4 leads to a very significant inhibition of cell differentiation, as demonstrated by significant changes in expression of the markers for pluripotency and cell differentiation in both hESCs and mESCs (Figure 7F).

DISCUSSION

In summary, we discovered a new feature of ESCs that provides a mechanistic explanation for the very early events that accompany induction of ESC differentiation (see the model in Figure 7G). We propose that differentiation signals induce significant changes in the structure of chromatin after DNA replication. Induction of h/mESC differentiation for 2 hr leads to accumulation of the H3K27me3 KDM UTX on nascent DNA (Figure 7). We propose that the activity of UTX overrides the activity of the HMT EZH2, causing a loss of this histone mark on nascent DNA for several hours after induction of mESC and hESC differentiation. Because H3K27me3 is a mark of condensed chromatin structure (Yuan et al., 2012), the early post-replicative chromatin of the induced h/mESCs, which lacks H3K27me3, should be more accessible for recruitment of all simultaneously induced TFs to genomic loci, including those critical to specify cell fate. This novel model for differentiation proposes that induced TFs do not have to overcome a chromatin barrier but, instead, gain access to their binding sites because of the decondensation of chromatin on nascent DNA.

An important conclusion of this study is that, following induction of h/mESC differentiation, the delay in accumulation of H3K27me3 after DNA replication was detected in the vast majority of individual cells analyzed by CAA, suggesting that it occurs in all replicating regions of the genome. A similar delay was also observed by re-ChIP assays at all examined H3K27me3-containing genes, which are likely replicating at different times during S phase. Because replication is unsynchronized in higher eukaryotes, our results suggest that the delay in the post-replicative accumulation of H3K27me3 occurs at all regions of the genome

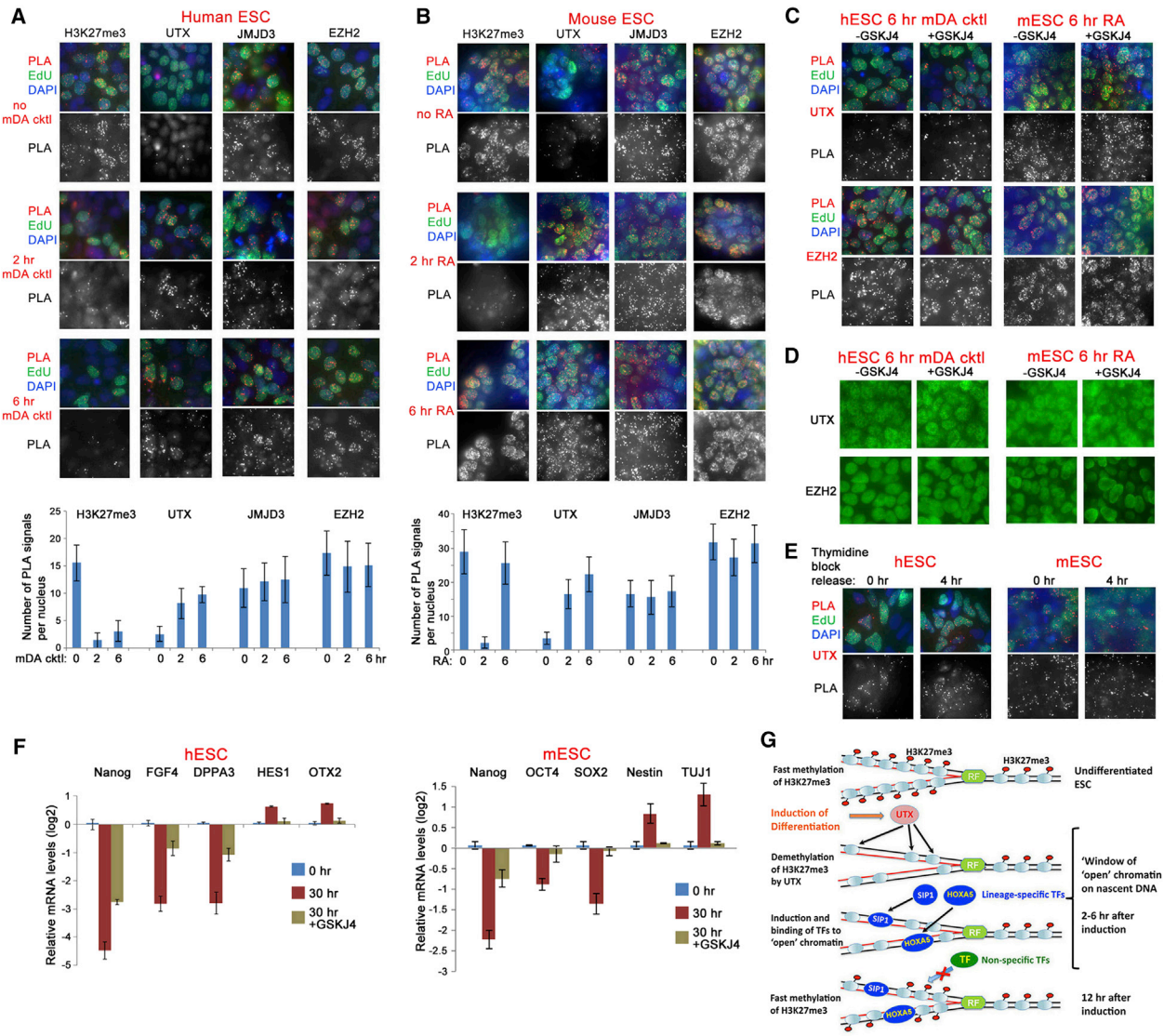

Figure 7. Association of H3K27me3 HMT and KDMs with DNA during Induction of Differentiation of mESCs and hESCs

(A) hESCs were grown in stage 1 medium for 4 days (top) and then induced to the mDA lineage for 2 hr (center) and 6 hr (bottom). Cells were labeled with EdU for 15 min, and CAA was performed for H3K27me3, UTX, JMJD3, and EZH2, followed by immunostaining for biotin (green). PLA only is shown in black and white.

(B) mESCs were grown for 2 days with LIF/2i (top) and then induced with RA for 2 hr (center) and 6 hr (bottom). Cells were labeled with EdU for 15 min, and CAA was performed for H3K27me3, UTX, JMJD3, and EZH2, followed by immunostaining for biotin (green). PLA only is shown in black and white.

In (A) and (B), quantification of the results of three independent CAA experiments is shown below.

(C) hESCs and mESCs were induced with mDA and RA, respectively, in the presence and absence of GSKJ4 (10 and 5 μM for hESCs and mESCs, respectively). Cells were labeled with EdU for 15 min, and CAA was performed for UTX and EZH2, followed by immunostaining for biotin (green). PLA only is shown in black and white.

(D) hESCs and mESCs were induced as in (C). Cells were immunostained with antibodies to UTX and EZH2.

(E) hESCs and mESCs were labeled, induced, and grown in the presence of thymidine as shown in Figure 5. The thymidine block was released for 4 hr. CAA was performed for UTX, followed by immunostaining for biotin (green). PLA only is shown in black and white.

(F) qRT-PCR analysis of the expression of pluripotency and differentiation markers in hESCs (left) and mESCs (right). Undifferentiated cells (0 hr) were induced with mDA and RA for 30 hr, respectively, in the absence and presence of 10 and 5 μM GSKJ4, respectively. The following pluripotency markers were tested: NANOG, FGF4, and DPPA3 in hESCs and NANOG, OCT4, and SOX2 in mESCs. The following differentiation markers were tested: HES1 and OTX2 in hESCs and Nestin and TUJ1 in mESCs.

(G) A model for the role of post-replicative chromatin for the association of lineage-specific TFs following induction of ESC differentiation. In un-induced ESCs, H3K27me3-containing chromatin with a high density of nucleosomes prevents binding of unwanted TFs (first row). Following induction of differentiation, de-methylation of H3K27me3 by induced UTX leads to a decrease in nucleosome spacing (second row). This "opening" of chromatin facilitates binding of the newly induced lineage-specific TFs (third row). The return of the fast mode of accumulation of H3K27me3 correlates with condensing nucleosome spacing, preventing further association of non-specific TFs which may cause changes in lineage commitment (fourth row).

as each replicon undergoes DNA replication. This conclusion agrees with previous studies that suggested that post-replicative DNA is more accessible to nucleases but that histones are still present (Galili et al., 1983; Seale, 1978).

Although pioneer TFs are able to bind DNA in the presence of nucleosomes (Cirillo et al., 2002; Iwafuchi-Doi and Zaret, 2014; Smale, 2010; Soufi et al., 2015; Voss and Hager, 2014), they cannot overcome the barrier of the H3K27me3-marked condensed chromatin (Iwafuchi-Doi and Zaret, 2016). The results of this work provide an explanation of how pioneer TFs like FOXA2 can efficiently bind to DNA of post-replicative chromatin lacking the H3K27me3 mark. Moreover, where KDM activities were inhibited (Figure 6) or progression into S phase was blocked (Figure 5), the pioneer factor FOXA2 (Sekiya et al., 2009) could not bind nascent DNA. Blocking KDM activities also resulted in marked inhibition of h/mESC differentiation, demonstrating the functional significance of the proposed mechanism for cell differentiation (Figure 7F). Interestingly, TFs that have previously not been identified as pioneer factors on reconstituted chromatin or bulk chromatin are also able to efficiently bind post-replicative chromatin with low levels of H3K27me3. We propose that, following induction of differentiation, all regions of replicating DNA will sequentially have low levels of H3K27me3, making all DNA binding sites available for recruitment of all newly induced TFs.

The decrease in the expression of pluripotency genes and induction of the pan-neural and subtype-specifying genes occurs much earlier than demonstrated previously, suggesting that early lineage decisions may occur within the first 6–12 hr of differentiation (Figures 3 and 4). Because all tested differentiation-specifying TFs are expressed within the period of low H3K27me3 post-replicative chromatin, we propose that this is beneficial for recruitment of these proteins to the loci they regulate to specify cell fate. Our data showing that an increase in post-replicative H3K27me3 or preventing DNA replication blocks recruitment of TFs to DNA (Figures 5 and 6) support this proposed model. It is interesting that the rate of accumulation of H3K27me3 significantly increases at or after 6 hr of induction of differentiation in both mESCs and hESCs, respectively. We speculate that, before and after the period of open post-replicative chromatin, the structure of chromatin may prevent association with DNA of unwanted transcription factors (Figure 7G). This may be essential for keeping cells in the pluripotent state or to preserve lineage commitment so that original choices are not overwritten by new TFs binding DNA during later stages of differentiation. Thus, these findings suggest the existence of a short ''window of opportunity'' soon after induction of cell differentiation, when more accessible, open nascent chromatin is available for association of the newly induced lineage-specifying TFs.

Our results correlate well with the functional analyses of the role of the cell cycle phases in the differentiation of stem cells. It is suggested that induction of differentiation and loss of pluripotency may represent two aspects of the same process that are intrinsically linked (Vallier, 2015). Although induction of stem cell differentiation to different lineages occurs in early and late G1 phase (Pauklin and Vallier, 2013), loss of ESC pluripotency is achieved subsequently in S and G2 phases (Gonzales et al., 2015). In molecular terms, induction of differentiation may represent induction of the primary transcription factors in response to signaling molecules, and loss of pluripotency may reflect the ability of these induced TFs to bind to their sites at repressed genes, activation of which is essential for loss of pluripotency of ESCs. The results of this study suggest that this second step is controlled by the structure of chromatin in early S phase. This is in line with the finding that epigenetic components are essential for the normal transition between pluripotency and differentiation (Gonzales et al., 2015). Together, these results could provide a molecular model of cell fate specification following induction of differentiation.

The newly found decondensed structure of post-replicative chromatin and its importance for acquiring differentiation signals in the form of binding of key TFs to DNA are likely the features of not only pluripotent but also multipotent cells, like hematopoietic blood progenitor cells (HPCs) (Petruk et al., 2017). Interestingly, the overall features of the open, H3K27me3-lacking chromatin are essentially the same in induced m/hESCs and HPCs, suggesting that this may be a general feature of all differentiating eukaryotic stem cells. These findings define a chromatin-based mechanism that explains the difference in phenotypic plasticity between stem/progenitor cells and differentiated cells. The results of our recent experiments suggest that human induced pluripotent stem cells (iPSCs) also possess a similar delay in accumulation of H3K27me3 during induction to the mDA lineage (J.C. and L.I., unpublished data). Thus, the discovery of a new chromatin-based mechanism that is essential for the early stages of lineage commitment in ESCs may also significantly affect our ability to direct the differentiation of patient-derived iPSCs into specific cell lineages, enabling the study and treatment of many different diseases.

STAR★METHODS

Detailed methods are provided in the online version of this paper and include the following:

- KEY RESOURCES TABLE
- CONTACT FOR REAGENT AND RESOURCE SHARING
- METHOD DETAILS
  - Maintenance and induction of differentiation of hESCs and mESCs
  - Chromatin Assembly Assay
  - Re-ChIP assays
  - Block of DNA replication
  - Inhibition of H3K27me3 KDMs by GSKJ4
  - Gene expression analysis by RT-qRCR
  - Dilutions of antibodies used
- DATA AND SOFTWARE AVAILABILITY

AUTHOR CONTRIBUTIONS

S.P., S.K.K., and G.S. performed the CAA studies. J.C., S.P., and R.S. performed the analysis of differentiation of hESCs and mESCs. A.M., S.P., J.C., L.I., H.W.B., and S.B.M. designed the study and wrote the manuscript. S.A.M. and B.C. discussed the results and designed the experiments. All authors commented on the manuscript.

ACKNOWLEDGMENTS

This work was supported by the following grants: NIH R01GM075141 (to A.M. and S.B.M.); NIH R01HL127895 (to A.M. and B.C.); NIH R01AI125650 (to A.M. and L.I.); NIH NS075839, the Parkinson's Council, and the Strauss Foundation (to L.I.); and a grant from the CIHR (to H.B.).

Received: August 24, 2016
Revised: December 28, 2016
Accepted: March 7, 2017
Published: April 11, 2017

REFERENCES

Al Tanoury, Z., Gaouar, S., Piskunov, A., Ye, T., Urban, S., Jost, B., Keime, C., Davidson, I., Dierich, A., and Rochette-Egly, C. (2014). Phosphorylation of the retinoic acid receptor RARγ2 is crucial for the neuronal differentiation of mouse embryonic stem cells. J. Cell Sci. *127*, 2095–2105.

Alabert, C., Bukowski-Wills, J.C., Lee, S.B., Kustatscher, G., Nakamura, K., de Lima Alves, F., Menard, P., Mejlvang, J., Rappsilber, J., and Groth, A. (2014). Nascent chromatin capture proteomics determines chromatin dynamics during DNA replication and identifies unknown fork components. Nat. Cell Biol. *16*, 281–293.

Barta, T., Dolezalova, D., Holubcova, Z., and Hampl, A. (2013). Cell cycle regulation in human embryonic stem cells: links to adaptation to cell culture. Exp. Biol. Med. (Maywood) *238*, 271–275.

Bell, O., Schwaiger, M., Oakeley, E.J., Lienert, F., Beisel, C., Stadler, M.B., and Schübeler, D. (2010). Accessibility of the Drosophila genome discriminates PcG repression, H4K16 acetylation and replication timing. Nat. Struct. Mol. Biol. *17*, 894–900.

Bonasio, R., Tu, S., and Reinberg, D. (2010). Molecular signals of epigenetic states. Science *330*, 612–616.

Cai, J., Donaldson, A., Yang, M., German, M.S., Enikolopov, G., and Iacovitti, L. (2009). The role of Lmx1a in the differentiation of human embryonic stem cells into midbrain dopamine neurons in culture and after transplantation into a Parkinson's disease model. Stem Cells *27*, 220–229.

Cai, J., Schleidt, S., Pelta-Heller, J., Hutchings, D., Cannarsa, G., and Iacovitti, L. (2013). BMP and TGF-β pathway mediators are critical upstream regulators of Wnt signaling during midbrain dopamine differentiation in human pluripotent stem cells. Dev. Biol. *376*, 62–73.

Chung, S., Leung, A., Han, B.S., Chang, M.Y., Moon, J.I., Kim, C.H., Hong, S., Pruszak, J., Isacson, O., and Kim, K.S. (2009). Wnt1-lmx1a forms a novel autoregulatory loop and controls midbrain dopaminergic differentiation synergistically with the SHH-FoxA2 pathway. Cell Stem Cell *5*, 646–658.

Cirillo, L.A., Lin, F.R., Cuesta, I., Friedman, D., Jarnik, M., and Zaret, K.S. (2002). Opening of compacted chromatin by early developmental transcription factors HNF3 (FoxA) and GATA-4. Mol. Cell *9*, 279–289.

Corpet, A., and Almouzni, G. (2009). Making copies of chromatin: the challenge of nucleosomal organization and epigenetic information. Trends Cell Biol. *19*, 29–41.

Filipczyk, A.A., Laslett, A.L., Mummery, C., and Pera, M.F. (2007). Differentiation is coupled to changes in the cell cycle regulatory apparatus of human embryonic stem cells. Stem Cell Res. (Amst.) *1*, 45–60.

Francis, N.J., Follmer, N.E., Simon, M.D., Aghia, G., and Butler, J.D. (2009). Polycomb proteins remain bound to chromatin and DNA during DNA replication in vitro. Cell *137*, 110–122.

Galili, G., Levy, A., and Jakob, K.M. (1983). Changes in chromatin structure at the replication fork. DNase I and trypsin-micrococcal nuclease effects on approximately 300- and 150-base pair nascent DNAs. J. Biol. Chem. *258*, 11274–11279.

Gonzales, K.A., Liang, H., Lim, Y.S., Chan, Y.S., Yeo, J.C., Tan, C.P., Gao, B., Le, B., Tan, Z.Y., Low, K.Y., et al. (2015). Deterministic restriction on pluripotent state dissolution by cell-cycle pathways. Cell *162*, 564–579.

Gualdi, R., Bossard, P., Zheng, M., Hamada, Y., Coleman, J.R., and Zaret, K.S. (1996). Hepatic specification of the gut endoderm in vitro: cell signaling and transcriptional control. Genes Dev. *10*, 1670–1682.

Iwafuchi-Doi, M., and Zaret, K.S. (2014). Pioneer transcription factors in cell reprogramming. Genes Dev. *28*, 2679–2692.

Iwafuchi-Doi, M., and Zaret, K.S. (2016). Cell fate control by pioneer transcription factors. Development *143*, 1833–1837.

Jonk, L.J., de Jonge, M.E., Kruyt, F.A., Mummery, C.L., van der Saag, P.T., and Kruijer, W. (1992). Aggregation and cell cycle dependent retinoic acid receptor mRNA expression in P19 embryonal carcinoma cells. Mech. Dev. *36*, 165–172.

Kapinas, K., Grandy, R., Ghule, P., Medina, R., Becker, K., Pardee, A., Zaidi, S.K., Lian, J., Stein, J., van Wijnen, A., and Stein, G. (2013). The abbreviated pluripotent cell cycle. J. Cell. Physiol. *228*, 9–20.

Kharchenko, P.V., Alekseyenko, A.A., Schwartz, Y.B., Minoda, A., Riddle, N.C., Ernst, J., Sabo, P.J., Larschan, E., Gorchakov, A.A., Gu, T., et al. (2011). Comprehensive analysis of the chromatin landscape in Drosophila melanogaster. Nature *471*, 480–485.

Kriks, S., Shim, J.W., Piao, J., Ganat, Y.M., Wakeman, D.R., Xie, Z., Carrillo-Reid, L., Auyeung, G., Antonacci, C., Buch, A., et al. (2011). Dopamine neurons derived from human ES cells efficiently engraft in animal models of Parkinson's disease. Nature *480*, 547–551.

Kruidenier, L., Chung, C.W., Cheng, Z., Liddle, J., Che, K., Joberty, G., Bantscheff, M., Bountra, C., Bridges, A., Diallo, H., et al. (2012). A selective jumonji H3K27 demethylase inhibitor modulates the proinflammatory macrophage response. Nature *488*, 404–408.

Kundaje, A., Meuleman, W., Ernst, J., Bilenky, M., Yen, A., Heravi-Moussavi, A., Kheradpour, P., Zhang, Z., Wang, J., Ziller, M.J., et al.; Roadmap Epigenomics Consortium (2015). Integrative analysis of 111 reference human epigenomes. Nature *518*, 317–330.

Li, V.C., Ballabeni, A., and Kirschner, M.W. (2012). Gap 1 phase length and mouse embryonic stem cell self-renewal. Proc. Natl. Acad. Sci. USA *109*, 12550–12555.

Mummery, C.L., van den Brink, C.E., and de Laat, S.W. (1987). Commitment to differentiation induced by retinoic acid in P19 embryonal carcinoma cells is cell cycle dependent. Dev. Biol. *121*, 10–19.

Murray, A.W., and Kirschner, M.W. (1989). Dominoes and clocks: the union of two views of the cell cycle. Science *246*, 614–621.

Pan, G., Tian, S., Nie, J., Yang, C., Ruotti, V., Wei, H., Jonsdottir, G.A., Stewart, R., and Thomson, J.A. (2007). Whole-genome analysis of histone H3 lysine 4 and lysine 27 methylation in human embryonic stem cells. Cell Stem Cell *1*, 299–312.

Pauklin, S., and Vallier, L. (2013). The cell-cycle state of stem cells determines cell fate propensity. Cell *155*, 135–147.

Petruk, S., Sedkov, Y., Johnston, D.M., Hodgson, J.W., Black, K.L., Kovermann, S.K., Beck, S., Canaani, E., Brock, H.W., and Mazo, A. (2012). TrxG and PcG proteins but not methylated histones remain associated with DNA through replication. Cell *150*, 922–933.

Petruk, S., Black, K.L., Kovermann, S.K., Brock, H.W., and Mazo, A. (2013). Stepwise histone modifications are mediated by multiple enzymes that rapidly associate with nascent DNA during replication. Nat. Commun. *4*, 2841.

Petruk, S., Mariani, S.A., De Dominici, M., Porazzi, P., Minieri, V., Cai, J., Iacovitti, L., Flomenberg, N., Calabretta, B., and Mazo, A. (2017). Structure of nascent chromatin is essential for hematopoietic lineage specification. Cell Rep. Published online April 11, 2017. http://dx.doi.org/10.1016/j.celrep.2017.03.035.

Prakash, N., and Wurst, W. (2007). A Wnt signal regulates stem cell fate and differentiation in vivo. Neurodegener. Dis. *4*, 333–338.

Rochette-Egly, C. (2015). Retinoic acid signaling and mouse embryonic stem cell differentiation: Cross talk between genomic and non-genomic effects of RA. Biochim. Biophys. Acta *1851*, 66–75.

Seale, R.L. (1978). Nucleosomes associated with newly replicated DNA have an altered conformation. Proc. Natl. Acad. Sci. USA *75*, 2717–2721.

Sekiya, T., Muthurajan, U.M., Luger, K., Tulin, A.V., and Zaret, K.S. (2009). Nucleosome-binding affinity as a primary determinant of the nuclear mobility of the pioneer transcription factor FoxA. Genes Dev. *23*, 804–809.

Sha, K., and Boyer, L.A. (2008). The chromatin signature of pluripotent cells. In StemBook (Harvard Stem Cell Institute).

Shlyueva, D., Stampfel, G., and Stark, A. (2014). Transcriptional enhancers: from properties to genome-wide predictions. Nat. Rev. Genet. *15*, 272–286.

Simandi, Z., Balint, B.L., Poliska, S., Ruhl, R., and Nagy, L. (2010). Activation of retinoic acid receptor signaling coordinates lineage commitment of spontaneously differentiating mouse embryonic stem cells in embryoid bodies. FEBS Lett. *584*, 3123–3130.

Singh, A.M., and Dalton, S. (2009). The cell cycle and Myc intersect with mechanisms that regulate pluripotency and reprogramming. Cell Stem Cell *5*, 141–149.

Sirbu, B.M., Couch, F.B., and Cortez, D. (2012). Monitoring the spatiotemporal dynamics of proteins at replication forks and in assembled chromatin using isolation of proteins on nascent DNA. Nat. Protoc. *7*, 594–605.

Smale, S.T. (2010). Pioneer factors in embryonic stem cells and differentiation. Curr. Opin. Genet. Dev. *20*, 519–526.

Soufi, A., Garcia, M.F., Jaroszewicz, A., Osman, N., Pellegrini, M., and Zaret, K.S. (2015). Pioneer transcription factors target partial DNA motifs on nucleosomes to initiate reprogramming. Cell *161*, 555–568.

Vallier, L. (2015). Cell cycle rules pluripotency. Cell Stem Cell *17*, 131–132.

Voss, T.C., and Hager, G.L. (2014). Dynamic regulation of transcriptional states by chromatin and transcription factors. Nat. Rev. Genet. *15*, 69–81.

Yuan, W., Wu, T., Fu, H., Dai, C., Wu, H., Liu, N., Li, X., Xu, M., Zhang, Z., Niu, T., et al. (2012). Dense chromatin activates Polycomb repressive complex 2 to regulate H3 lysine 27 methylation. Science *337*, 971–975.

Zaret, K. (1999). Developmental competence of the gut endoderm: genetic potentiation by GATA and HNF3/fork head proteins. Dev. Biol. *209*, 1–10.

Zaret, K.S., and Carroll, J.S. (2011). Pioneer transcription factors: establishing competence for gene expression. Genes Dev. *25*, 2227–2241.

STAR★METHODS

KEY RESOURCES TABLE

REAGENT or RESOURCE	SOURCE	IDENTIFIER
Antibodies		
Rabbit polyclonal anti-SIP1	Sigma-Aldrich	Cat#HPA003456; RRID: AB_10603840
Rabbit polyclonal anti-LMX1A	Dr. German	N/A
Goat polyclonal anti-FOXA2	R&D Systems	Cat# AF2400; RRID: AB_2294104
Mouse monoclonal anti-SOX2	R&D Systems	Cat# MAB2018; RRID: AB_358009
Goat polyclonal anti-OCT4	R&D Systems	Cat# AF1759; RRID: AB_354975
Mouse monoclonal anti-SSEA4	DSHB	Cat# MC-813-70; RRID: AB_528477
Rabbit polyclonal anti-RAR beta	Abcam	Cat#ab53161; RRID: AB_882283
Rabbit polyclonal anti-HOXA3	Sigma-Aldrich	Cat#H3791; RRID: AB_10621818
Rabbit polyclonal anti-HOXA5	Abgent	Cat#AP6694B; RRID: AB_1967798
Rabbit monoclonal anti-Ezh2	Cell Signaling Technology	Cat# 5246; RRID: AB_10694683
Rabbit polyclonal anti-Trimethyl-Histone H3(Lys27)	Millipore	Cat#07-449; RRID: AB_310624
Rabbit polyclonal anti-UTX	Thermo Fisher Scientific	Cat#PA5-31828; RRID: AB_2549301
Rabbit polyclonal anti-JMJD3	Thermo Fisher Scientific	Cat#PA5-22974; RRID: AB_11151839
Goat polyclonal anti-biotin	Vector Laboratories	Cat#SP-3000; RRID: AB_2336111
Mouse monoclonal anti-biotin	Jackson ImmunoResearch	Cat#200-002-211; RRID: AB_2339006
Rabbit polyclonal anti-biotin	Abcam	Cat#ab1227; RRID: AB_298990
Mouse monoclonal anti-BrdU	Exbio	Cat#11-286-C100; RRID: AB_10732986
Mouse monoclonal anti-BrdU	BD Biosciences	Cat#555627; RRID: AB_395993
Donkey anti-mouse Alexa Fluor 488 secondary	Jackson ImmunoResearch	Cat#715-545-150; RRID: AB_2340846
Donkey anti-goat Alexa Fluor 488 secondary	Jackson ImmunoResearch	Cat#705-545-147; RRID: AB_2336933
Donkey anti-rabbit Alexa Fluor 488 secondary	Jackson ImmunoResearch	Cat#711-095-152; RRID: AB_2315776
Mouse anti-biotin Alexa Fluor 488 secondary	Jackson ImmunoResearch	Cat#200-542-211; RRID: AB_2339040
Rabbit IgG	Jackson ImmunoResearch	Cat#011-000-003; RRID: AB_2337118
Rabbit anti-mouse IgG	Jackson ImmunoResearch	Cat#315-005-045; RRID: AB_2340038
Chemicals, Peptides, and Recombinant Proteins		
SB431452	Tocris	Cat# 1614
Dorsmorphin	Tocris	Cat# 3093
Purmorphamine	Stemgent	Cat# 04-0009
Recombinant Human Sonic Hedgehog/Shh Protein	R&D Systems	Cat#8908-SH
Recombinant Human/Mouse FGF-8b Protein	R&D Systems	Cat# 423-F8
mTeSR1	Stem Cell Technology	Cat# 05850
KOSR	Thermo Fisher Scientific	Cat# 10828028
N2	Thermo Fisher Scientific	Cat#17502048
B27	Thermo Fisher Scientific	Cat#17504044
DMEM	Corning Cellgro	Cat#15-017-CV
Fetal Bovine Serum	Gemini Bio-Product	Cat#100-500
HEPES	Corning	Cat#25-060-CI
MEM Nonessential Amino Acid	Corning	Cat#25-025-CI
L-glutamine	Corning	Cat#25-005-CI
PD0325901	Selleckchem	Cat#S1036
CHIR99021	Selleckchem	Cat#S1263
Mouse Leukemia Inhibitory Factor	Gemini Bio-Product	Cat#400-495
Retinoic Acid	Sigma-Aldrich	Cat#R2625

(*Continued on next page*)

Continued

REAGENT or RESOURCE	SOURCE	IDENTIFIER
EdU	Invitrogen	Cat#A10044
Biotin Azide	Invitrogen	Cat#B10184
BrdU	Sigma-Aldrich	Cat#B5002
Protein G agarose	Millipore	Cat#16-2012
Thymidine	Sigma-Aldrich	Cat#T9250
GSK J4	Tocris	Cat#4594
TRIzol	Thermo Fisher Scientific	Cat#15596018
Critical Commercial Assays		
Click-iT Cell Reaction Buffer Kit	Invitrogen	Cat#C10269
High Pure RNA Isolation Kit	Roche	Cat#11828665001
Superscript III Reverse Transcriptase	Invitrogen	Cat#18080085
SYBR Green PCR Master Mix	TheroFisher Scientific	Cat#4309155
Duolink In Situ detection Reagent Red	Sigma-Aldrich	Cat#DUO92008
Duolink In Situ PLA Probe anti-Rabbit Minus	Sigma-Aldrich	Cat#DUO92005
Duolink In Situ PLA Probe anti-mouse Plus	Sigma-Aldrich	Cat#DUO92001
Duolink In Situ PLA Probe anti-goat Plus	Sigma-Aldrich	Cat#DUO92003
Deposited Data		
Image data	Mendeley	http://dx.doi.org/10.17632/drhrkf7w2c.1
Experimental Models: Cell Lines		
Human: H9	WiCell	Cat# WA09; RRID: CVCL_9773
Mouse: E14TG2a	ATCC	Cat#CRL-1821; RRID: CVCL_9108
Oligonucleotides		
hDPPA3 Forward: 5′ TGTTACTCGGCGGAGTTCGTAC 3′	IDT	N/A
hDPPA3 Reverse: 5′ GATCCCATCCATTAGACACGCAG 3′	IDT	N/A
hFGF4 Forward: 5′ CGTGGTGAGCATCTTCGGCGT 3′	IDT	N/A
hFGF4 Reverse: 5′ GTAGGACTCGTAGGCGTTGTAG 3′	IDT	N/A
hFOXA2 Forward: 5′ GGAACACCACTACGCCTTCAAC 3′	IDT	N/A
hFOXA2 Reverse: 5′ AGTGCATCACCTGTTCGTAGGC 3′	IDT	N/A
hGAPDH Forward: 5′GGAGTCAACGGATTTGGTCGTA 3′	IDT	N/A
hGAPDH Reverse: 5′GAATTTGCCATGGGTGGAAT 3′	IDT	N/A
hHES1 Forward: 5′ GGAAATGACAGTGAAGCACCTCC3′	IDT	N/A
hHES1 Reverse: 5′ GAAGCGGGTCACCTCGTTCATG 3′	IDT	N/A
hLMX1A Forward: 5′CATCGAGCAGAGTGTCTACAGC 3′	IDT	N/A
hLMX1A Reverse: 5′ TGTCGTCGCTATCCAGGTCATG 3′	IDT	N/A
hNANOG Forward: 5′ CTCCAACATCCTGAACCTCAGC 3′	IDT	N/A
hNANOG Reverse: 5′ CGTCACACCATTGCTATTCTTCG3′	IDT	N/A
hNESTIN Forward: 5′ GCGGCTGCGGGCTACTGAAA 3′	IDT	N/A
hNESTIN Reverse: 5′ GCCACCTCCAGGCTGAGGGA 3′	IDT	N/A
hOCT4 Forward: 5′ AGTACCCGTCGCTGCACTCCA 3′	IDT	N/A
hOCT4 Reverse: 5′TTGCCCTGGGACACGGCGATG 3′	IDT	N/A
hOTX2 Forward: 5′ GGAAGCACTGTTTGCCAAGACC 3′	IDT	N/A
hOTX2 Reverse: 5′ CTGTTGTTGGCGGCACTTAGCT 3′	IDT	N/A
hPAX6 Forward: 5′CTGAGGAATCAGAGAAGACAGGC3′	IDT	N/A
hPAX6 Reverse: 5′ATGGAGCCAGATGTGAAGGAGG 3′	IDT	N/A
hSIP1 Forward: 5′AATGCACAGAGTGTGGCAGAGGC3′	IDT	N/A
hSIP1 Reverse: 5′CTGCTGATGTGCGAACTGTAGG 3′	IDT	N/A
hSOX1 Forward: 5′ AGTCTGGCCCCTGTGCTCCC 3′	IDT	N/A
hSOX1 Reverse: 5′ CCCGGGCGCACTAACTCAGC 3′	IDT	N/A

(*Continued on next page*)

Continued

REAGENT or RESOURCE	SOURCE	IDENTIFIER
mGAPDH Forward: 5′ GGAAAGCTGTGGCGTGAT 3′	IDT	N/A
mGAPDH Reverse: 5′TCAGCTCTGGGATGACCTT	IDT	N/A
mHoxa3 Forward: 5′ TGCCAACAGCAACCCTAC 3′	IDT	N/A
mHoxa3 Reverse: 5′ CTGCCTTGACTCTTTCATCCA 3′	IDT	N/A
mHoxa5 Forward: 5′ GCGCAAGCTGCACATTAG 3′	IDT	N/A
mHoxa5 Reverse: 5′ CGGTTGAAGTGGAATTCTTTCTC 3′	IDT	N/A
mNanog Forward: 5′ TCCTGAACTACTCTGTGACTCC 3′	IDT	N/A
mNanog Reverse: 5′ CTGGCTTTGCCCTGACTTTA 3′	IDT	N/A
mNestin Forward: 5′ TTGCAGACACCTGGAAGAAG 3′	IDT	N/A
mNestin Reverse: 5′ CCTCTGGTATCCCAAGGAAATG 3′	IDT	N/A
mOct4 Forward: 5′ GGCGTTCTCTTTGGAAAGGT 3′	IDT	N/A
mOct4 Reverse: 5′ CCGCAGCTTACACATGTTCTTA 3′	IDT	N/A
mRarb Forward: 5′ CTCAATCCATCGAGACACAGAG 3′	IDT	N/A
mRarb Reverse: 5′ AAACGAAGCAGGGCTTGTA 3′	IDT	N/A
mSOX2 Forward: 5′ AGCTACGCGCACATGAA 3	IDT	N/A
mSox2 Reverse: 5′ TGCATCGGTTGCATCTGT 3′	IDT	N/A
mTuj1 Forward: 5′ AAGACAAGCAGCATCTGTCC 3′	IDT	N/A
mTuj1 Reverse: 5′ CTTTAACCTGGGAGCCCTAATG 3′	IDT	N/A
ANXA9 Forward: 5′ TGGAGCCAGAGCAGAG 3′	IDT	N/A
ANXA9 Reverse: 5′ ACCACAGAGACCTAGTCTCAAA3′	IDT	N/A
KCNQ5 Forward: 5′ CCGCTGCTGAACTTCTCAA 3′	IDT	N/A
KCNQ5 Reverse: 5′ CGAAGCCTGGGAGAACAAA 3′	IDT	N/A
RETN Forward: 5′ GACCAGTCTCTGGACATGAAG 3′	IDT	N/A
RETN Reverse: 5′ ACATGAAGGGCTGGAGGA 3′	IDT	N/A
RGS6 Forward: 5′ ACACGTCAGTGAGGGAGAT 3′	IDT	N/A
RGS6 Reverse: 5′ CGCCGTCAAGGTTCTCTTAG 3′	IDT	N/A
TLR2 Forward: 5′ GCGCGGAGTTTCCCTTT 3′	IDT	N/A
TLR2 Reverse: 5′ CCTGGCTCGCCTTTCTC 3′	IDT	N/A
Software and Algorithms		
Adobe Photoshop	Adobe	RRID: SCR_014199

CONTACT FOR REAGENT AND RESOURCE SHARING

As Lead Contact, Alexander Mazo is responsible for all reagent and resource requests. Please contact Alexander Mazo at alexander.mazo@jefferson.edu with requests and inquiries.

METHOD DETAILS

Maintenance and induction of differentiation of hESCs and mESCs

hES cells (H9 cells, Passage 35–50) were purchased from Wicell Research Institute and maintained according to the supplier's instructions. Briefly, cells were grown as feeder free cells in mTesR1 medium. Cell propagation was achieved through manual dissection and transfer of cut cell colonies once every 3-5 days. The differentiation process was initiated by treating them with DMEM/F12 media (supplemented with 20% Knockout Serum Replacer, 1% Non-Essential Amino Acids, 0.1 mM 2-mercaptoethanol, 4 ng/ml bFGF, two TGF/BMP inhibitors SB431542 (10 μM) and Dorsomorphin (2 μM) and SHH (C24II) (100 ng/ml), the SHH agonist Purmorphamine (2 μM) for 1 week. Then neural progenitors (NPs) were generated in N2/B27 NEP-basal medium supplemented with 100 ng/ml FGF8 and 200 nM Pur.

mES cells (E14TG2a) were cultured in feeder-free conditions on gelatinized tissue culture plates in high glucose DMEM supplemented with 15% FBS, 1X non-essential amino acids, 2mM L-glutamine, 10mM HEPES, 0.1mM 2-mercaptoethanol and, 1,000 U/ml LIF. Cell pluripotency was maintained by dual inhibition (2i) with 1 μM MEK inhibitor PD0325901 and 3 μM GSK3 inhibitor CHIR99021. For induction of differentiation cells were trypsinized, and plated on 0.1% gelatinizied chamber slides and grown for 2 days in LIF/2i medium. Cells were induced by changing to the medium without LIF/2i and with addition of 2 μM all-trans RA.

Chromatin Assembly Assay

hESCs and mESCs were grown on chamber slides, pulse-labeled with 5 μM EdU and fixed at room temperature with 4% formaldehyde in PBS for 15 min, washed with PBS, and permeabilized with 0.3% Triton for 15 min. Cells were subjected to Click-iT reaction with biotin-azide for 30 min. The PLA reactions (Olink) between the anti-biotin antibody and antibodies to other proteins were performed as described by Olink. Following PLA, cells were immunostained with anti-biotin Alexa Fluor 488 antibody to control the specificity of CAA. The results of CAA experiments shown in Figure 1A were quantified by counting the number of PLA signals per EdU-labeled nuclei in 50 cells of each of the three independent experiments. The nature of the results in the rest of the figures alleviated the need to quantify the results of these assays.

Re-ChIP assays

2-4x10 ^{7} hESC were grown on 100 mm dishes, and half of the cells were induced for 2 hr 30 min with the mDA cocktail. Undifferentiated and induced cells were labeled with 50 μM BrdU for 12 min or 12 min followed by chase to 60 min, washed with PBS and fixed with 1% formaldehyde for 10 min at room temperature. After fixation glycine was added to final concentration of 0.125 M to quench formaldehyde. Cells were washed with PBS, scraped from plates, collected by centrifugation for 5 min at 1000 rpm at 4°C, re-suspended in 1 mL of RIPA buffer (1% Triton X-100, 0.1% sodium deoxycholate, 0.05% SDS, 0.15 M NaCl, 10 mM Tris-HCl, pH 8.0, 1 mM EDTA, pH 8.0) with protease inhibitor. Suspension was sonicated to sheare DNA to an average length of about 500-1000 bp and centrifuged for 5 min at 14,000 rpm. The supernatant was pre-cleared with protein-G agarose/Salmon Sperm DNA for 1 hr at 4°C. 5% of material was used as input, and the remaining material was divided for incubation overnight at 4°C with 30 μg of rabbit polyclonal anti-trimethyl H3K27 or with 30 μg of rabbit IgG as a control. The protein-G agarose/Salmon Sperm DNA was added for 1h, beads were collected by centrifugation and sequentially washed for 3 min in 1ml of low salt wash buffer (0.1% SDS, 1% Triton X-100, 2 mM EDTA, 20 mM Tris-HCl, pH 8.1, 150 mM NaCl), high salt wash buffer (0.1% SDS, 1% Triton X-100, 2 mM EDTA, 20 mM Tris-HCl, pH 8.1, 500 mM NaCl), LiCl wash buffer (0.25 M LiCl, 1% NP40, 1% deoxycholate, 1 mM EDTA, 10 mM Tris-HCl pH 8.1) and then twice with TE (10 mM Tris-HCl pH, 8.0, 1mM EDTA). Beads were incubated two times for 15 min in 250 μl of the elution buffer (1% SDS, 0.1 M $NaHCO_3$) at room temperature, supernatants were combined and incubated at 65°C for 16 hr in the presence of 0.2 M NaCl to reverse cross-link, and treated with proteinase K for 2 hr at 45°C. DNA was purified by phenol/chloroform extraction and precipitated with ethanol. DNA was re-suspended in 500 μl of the TE buffer. 5% of material was removed and used as second input in the analysis by real time PCR. 20 μg of salmon sperm DNA was added to the remaining material. Samples were boiled for 5 min and then kept on ice for 2 min. 50 μl of the 10xadjusting buffer (110 mM sodium phosphate, pH 7.0, 1.52 M NaCl, 0.55% Triton X-100) was added to samples. Samples were incubated at room temperature for 20 min with 15 μg of anti-brdU antibody (BD Biosciences), followed by 20 min incubation with 35 μg of rabbit anti-mouse IgG. Samples were centrifugated at 18,000 g for 20 min and pellet was washed with the adjusting buffer and incubated for 2 hr at 45°C in the lysis buffer (50 mM Tris-HCl, pH 8.0, 10 mM EDTA, 0.5% SDS, 25 mg/ml proteinase K). DNA was purified by phenol/chloroform, precipitated with ethanol and used for analysis. All PCR reactions were performed with an Applied Biosystems StepOne Real-Time PCR system.

Block of DNA replication

To block DNA replication, hESCs and mESCs were labeled with EdU for 30 min, induced to specific lineage for 24 hr in the presence of 2 mM thymidine. To restore DNA replication, thymidine was removed by washing, and cells were grown in culture media without thymidine for 4 hr, fixed, and analyzed by CAA with antibodies against biotin (EdU-labeled DNA) and corresponding TFs. The efficiency of the thymidine block of DNA replication was tested by labeling cells with 30 μM BrdU for 20 min in thymidine and after removal of thymidine, fixed with 4% formaldehyde, denatured in 2N hydrochloric acid for 20 min, washed in PBS and incubated with monoclonal anti-BrdU antibody (Exbio) followed by incubation with anti-mouse Alexa Fluor 488.

Inhibition of H3K27me3 KDMs by GSKJ4

To inhibit enzymatic activities of UTX and JMJD3 hESCs and mESCs were grown for 6 hr in the presence of 10 μM GSKJ4 dissolved in DMSO. DMSO without GSKJ4 was added in control experiments. See figure legends for conditions of particular experiments. Cells were then processed for CAA or collected for gene expression analysis. To test the effect of GSKJ4 on cell differentiation, undifferentiated hESCs were pretreated with 10 μM GSKJ4 for 12 hr, induced with the mDA cktl and grown for additional 30 hr in the presence of 10 μM GSKJ4. Undifferentiated mESCs were pretreated with 5 μM GSKJ4 for 6 hr, induced by adding RA and grown in the presence of 5 μM GSKJ4 for additional 48 hr. Cells treated with DMSO only were served as a control.

Gene expression analysis by RT-qRCR

Total RNA was isolated directly from freshly collected hESCs with TRIzol and for mESCs with High Pure RNA Isolation Kit. cDNA was synthesized by using 1 μg total RNA in a 20 μL reaction with Superscript III and oligo (dT) for hESC or random hexamers (Life Tech) for mECS. After reverse transcription was complete, one microliter of RNase H was added to each reaction tube, and the tubes were incubated for 20 min at 37°C before proceeding to PCR. Real-time PCR was carried out on a 7500 Real-Time PCR System using the 2x Power SYBR green PCR master mix. GAPDH was used as an internal control. All PCR products were checked by running an agarose gel for the first time and by doing dissociation assay every time to exclude the possibility of multiple products. PCR analyses were conducted in triplicate for each sample.

Dilutions of antibodies used

For PLA: rabbit anti SIP1 (1:200), rabbit anti LMX1A (1:200), goat anti FOXA2 (1:200), rabbit anti-RAR beta (1:200), rabbit anti-HOXA5 (1:200), rabbit anti-HOXA3 (1:100), rabbit anti-H3K27me3 (1:2500), mouse anti-biotin for hESCs (1:1000), goat anti-biotin for mESC (1:1000), rabbit anti-UTX (1:400), rabbit ani-JMJD3 (1:400), rabbit anti-EZH2 (1:400), mouse anti-BrdU (1:100).

For immunostaining of hESCs: anti-SOX2 (1:500), anti-OCT4 (1:100), anti-SSEA4 (1:50).

DATA AND SOFTWARE AVAILABILITY

Original imaging data have been deposited to Mendeley Data and are available at http://dx.doi.org/10.17632/drhrkf7w2c.1.